Portland, Oregon
NOISE-CON 2011
2011 July 25-27

Preliminary assessment of the interior noise environment in the Large Civil Tiltrotor (LCTR2)

Ferdinand W Grosveld[a)]
Lockheed Martin
Mail Stop 463
NASA Langley Research Center
Hampton, VA 23681

Randolph H Cabell[b)]
Mail Stop 463
NASA Langley Research Center
Hampton, VA 23681

The second-generation Large Civil Tiltrotor (LCTR2) serves as a representative vehicle under the NASA Fundamental Aeronautics Program (FAP) Subsonic Rotary Wing (SRW) project with a design goal to transport 90 passengers over a distance of 1800 km at a speed of 550 km/hr. The tiltrotor combines the vertical lift capability of a helicopter with the speed, altitude, and range of a turboprop airplane. The blade-passage frequency of the four-bladed rotor is as low as 6.9 Hz during cruise conditions. The resulting low-frequency acoustic excitation and its harmonics, combined with the anticipated use of lightweight composite and sandwich materials for the fuselage sidewall, may pose a challenge to achieving acceptable interior noise levels. The objective of the present study is to perform a preliminary assessment of the expected interior noise environment in the LCTR2 cabin. The approach includes a combination of semi-empirical, analytical, and statistical energy analysis methods. Because the LCTR2 is a notional vehicle, the prediction approach was also applied to the XV-15 tiltrotor and Bombardier Q400 turobprop aircraft to compare predictions with publicly available experimental data. Guidance for the expected interior noise levels in the LCTR2 was obtained by considering both the predicted exterior noise levels and the transmission loss of a basic fuselage sidewall consisting of a skin, porous layer and a trim panel. Structural and acoustic resonances are expected to coincide with low order harmonics of the blade passage frequency. The estimated sound pressure levels in the LCTR2 may not be acceptable when evaluated against known characteristics of human response to low frequency sound.

1 INTRODUCTION

The Large Civil Tiltrotor (LCTR) was developed under the NASA Heavy Lift Systems Investigation[1] as an economically competitive alternative to medium range regional airliners while significantly relieving runway and terminal area congestion. The second-generation

[a)] Email: f.grosveld@nasa.gov
[b)] Email: randolph.h.cabell@nasa.gov

configuration LCTR2 (Fig. 1) has a design goal to transport 90 passengers over a distance of 1800 km at a speed of 550 km/hr and serves as a representative vehicle design and mission under the NASA Fundamental Aeronautics Program (FAP) Subsonic Rotary Wing (SRW) project[2,3]. The tiltrotor design combines the speed, altitude and range of a turboprop airplane with the vertical lift capability of a helicopter freeing up existing runways for use by larger and longer-range aircraft. Several high risk areas have been identified for the LCTR configuration, such as the need for a high torque, low weight drive system and a high performance, structurally efficient rotor/wing system. In addition, the very low blade passage frequency of the four-bladed rotor (as low as 6.9 Hz during cruise conditions) and the anticipated use of lightweight composite and sandwich materials in the fuselage sidewall present unique challenges to achieving acceptable interior noise levels. The objective of the present study is to perform a preliminary assessment of the interior noise environment in the LCTR2 using existing prediction methods and data available in the literature.

2 ASSESSMENT APPROACH

Predicting the interior noise for the LCTR2 is a challenging task as the current vehicle description merely consists of an outer mold line without any structural details. In addition, the blade passage frequency in the cruise configuration is extremely low (6.9 Hz) and no experimental data exists for the vehicle to validate a numerical or analytical model. The assessment approach taken here is to first estimate the exterior sound pressure levels incident on the fuselage using an empirical near-field propeller prediction method. To gain confidence in this exterior prediction method, the approach is applied to a Bell Helicopter XV-15 tiltrotor (Fig. 2) and compared with publicly available exterior sound pressure level measurements performed on the vehicle during cruise flight conditions. In a second step, the sound transmission loss (TL) of a notional fuselage structure is predicted using analytical expressions and statistical energy analysis (SEA). Guidance for the expected interior noise levels in the LCTR2 is then obtained by considering both the predicted exterior noise levels and the fuselage transmission loss.

Although no detailed sidewall structure has yet been designed for the LCTR2, the proposed cabin arrangement is similar to a stretched version[4] of the Bombardier Q400 turboprop aircraft (Fig. 3), designated the Q400x. Hence, to enable this preliminary noise assessment, the fuselage sidewall including the dimensions and spacing of the longitudinal stringers and ring frames of the Q400 was used as the baseline structure for the LCTR2. Furthermore, interior noise levels are available for a Q400 aircraft during cruise flight conditions, thus providing additional measured data to benchmark the noise assessment approach described here. To use this measured interior noise data, a semi-empirical transmission loss of the Q400 fuselage sidewall was computed from the predicted exterior sound pressure levels incident on the fuselage, the publicly available measured interior sound pressure levels and the estimated absorption inside the cabin.

Geometric and operating design parameters for the LCTR2 tiltrotor, the Bombardier Q400 turboprop airliner and the Bell XV-15 tiltrotor are listed in Table 1.

3 NEAR-FIELD ROTOR NOISE ESTIMATES

Since much of the detailed information for the LCTR2 tiltrotor is yet unknown, an empirically-based prediction procedure for near-field propeller noise was used to estimate the noise levels on the surface of the fuselage. The procedure is based on existing propeller data and

is published in a SAE Aerospace Information Report[5]. The procedure computes incident sound pressure levels at the blade passage frequency and its harmonics from operating and installation parameters including flight speed, altitude, speed of sound, number of rotor blades, blade diameter, rotor speed, number of rotors, engine power, power absorbed by the rotor blades and distance from the rotor tip to the fuselage.

To gain confidence in the SAE prediction procedure, near field rotor noise predictions were made for the XV-15 tiltrotor flying at 370 km/hr at an altitude of 838 m for comparison with flight test data reported in Reference 6. The relevant flight test data consisted of exterior surface pressure measurements acquired at a flight speed of 370 km/hr and a propeller speed setting at a nominal 522 rotations per minute (rpm). The power of each engine was estimated to be 932 kW as input for the prediction procedure. The rotor speed of 523 rpm accounts for a rotational Mach number of 0.61 and a helical tip Mach number of 0.68. The measured and predicted sound pressure levels on the XV-15 tiltrotor fuselage surface are graphically compared in Fig. 5 at the fundamental rotor blade passage frequency and eleven harmonics. Good agreement was obtained for the rotor harmonics as the predictions are well within 3 dB of the measured data but not for the fundamental blade passage frequency at 26 Hz. It is not clear if the 12 dB discrepancy at this frequency is due to erroneous assumptions in the prediction or due to inaccuracies in the flight data acquisition. Broadband rotor noise was not predicted for this preliminary assessment.

Near-field propeller noise was predicted in the propeller plane of the Q400 turboprop aircraft at cruise flight conditions for which interior noise measurements are available.[7] The aircraft was flying 667 km/hr at an altitude of 7620 m. The standard atmosphere temperature at that altitude was -34.5 °C. These conditions resulted in a rotational blade tip Mach number of 0.59 and a helical Mach number of 0.84. The continuous power to the propeller was estimated to be 3620 kW. The estimated sound pressure levels in the propeller plane on the surface of the Q400 fuselage at the fundamental rotor blade passage frequency and the first twelve harmonics are shown in Fig. 6. No exterior pressure measurements are available for this aircraft for comparison with the prediction.

Near-field rotor noise of the LCTR2 was estimated for cruise flight conditions at a speed of 556 km/hr, an altitude of 8534 m, outside temperature of -40.7 °C, rotational Mach number of 0.35 and a helical Mach number of 0.61. The power of each engine was assumed to be 10067 kW. The predicted fuselage surface sound pressure levels at the blade passage frequency and first twelve harmonics are shown in Fig. 6. The validity of extending the SAE prediction procedure to the LCTR2 may be open for discussion since the rotor diameter, tip-fuselage clearance, and high engine power rating of the LCTR2 are outside the empirical database used to create the SAE procedure. In addition, the poor agreement between the predicted and the measured level for the blade passage frequency of the XV-15 indicates reason for caution. Nonetheless, the output of the SAE method was used in this study in the absence of any other proven prediction approach. Future work will investigate predictions from a computational fluid dynamics (CFD)-based method.

The predicted fundamental and harmonic sound pressure levels of the Q400 and the LCTR2 are compared in Fig. 6 for their respective cruise flight conditions. The exterior pressure fields are dominated by the blade passage frequency, although it should be noted that the predicted levels of the higher harmonics of the LCTR2 field are more than 10 dB below the level of the blade passage frequency of the Q400. The lower frequencies of the LCTR2 blade passage

frequency and harmonics, when compared with the Q400, result in lower A-weighted sound pressure levels as indicated in Fig. 6. The comparison of the A-weighted levels, normally used to more accurately describe human response to acoustic exposure, should be treated with caution, as A-weighting is customarily not applied to infrasound (below 20 Hz).

4 SIDEWALL TRANSMISSION LOSS

The Q400 fuselage sidewall was chosen as the baseline sidewall for the LCTR2. The transmission loss of a Q400 sidewall cross-section was predicted using an analytical analysis and statistical energy analysis (SEA). The predictions were compared with a semi-empirical transmission loss derived from Q400 interior measurements at cruise flight conditions and the predicted exterior sound pressure levels from the SAE method described previously. The measured interior levels were available as overall levels for seats in the front, middle, and back of the cabin, and as one-third octave band levels for the front location[7]. The sound transmission loss of the Q400 sidewall cross-section was estimated by using the predicted external surface pressures, subtracting the measured interior sound pressure levels and adjusting for the sound absorption inside the cabin.

4.1 Notional Sidewall Configuration and Properties

For these predictions, the notional sidewall configuration was defined using geometry and material information of a Bombardier Dash-8 Q400 fuselage section described in Reference 8. The fuselage was 2.68 m in diameter with a 1.6 mm thick aluminum skin and a skin surface density of 4.35 kg/m^2. The fuselage was stiffened by evenly spaced ring frames and longitudinal stringers. Sandwich trim panels with 0.9 mm thick aluminum face sheets and a 6 mm thick aramid fiber honeycomb core were installed at a distance of 81 mm from the fuselage skin. The surface density of the honeycomb trim panel was 4.88 kg/m^2. The mechanical material properties of the honeycomb core are listed in Table 2. The space between the skin and the trim panel was filled by a porous absorptive material with the material properties listed in Table 3.

4.2 Analytical Panel Transmission Loss

Transmission loss of the fuselage skin alone, without the absorption material or the trim panel, was computed using an expression derived by Koval[9] for the transmission loss of a curved panel in the presence of flow and cabin pressurization. Koval considered a harmonic, oblique plane wave p_i incident on a panel in a fluid moving with mean Mach number M. The flow is aligned with the longitudinal x axis and the pressure wave p_i is incident on the panel with elevation angle φ_1 and azimuth angle β. The transmitted pressure wave propagates with elevation angle φ_2 and azimuth angle β. The angles are illustrated in Figure 7 with the moving fluid on the incident side of the plate and the stationary fluid on the transmitted side of the plate.

The transmission loss across a shallow "infinite" cylindrical homogeneous panel with radius R, surface mass ρ_s, longitudinal stress σ_x and hoop stress σ_y due to pressurization p_p, is given for a complex elasticity modulus $E^*=E(1+i\eta)$ with loss factor η and with θ_1 and θ_2 being the compliments (measured from the normal to the panel) of the angles φ_1 and φ_2 by[9]

$$TL = 10\log\left(\left\{\left(\frac{\rho_2 c_2}{4\rho_1 c_1}\right)^{0.5} + \left(\frac{\rho_1 c_1}{4\rho_2 c_2}\right)^{0.5} \frac{\cos\theta_2}{\cos\theta_1\left(1+M\sin\theta_1\cos\beta\right)} + \right.\right.$$
$$+ \frac{\eta\rho_s\omega}{2\left(\rho_1 c_1 \rho_2 c_2\right)^{0.5}}\left[\frac{\omega^2}{\omega_{cr2}^2}\cos^4\theta_2 + \frac{\omega_R^2}{\omega^2}\cos^4\beta\right]\Bigg\}^2 + \qquad (1)$$
$$\left. + \left\{\frac{\rho_s\omega\cos\theta_2}{2\left(\rho_1 c_1 \rho_2 c_2\right)^{0.5}}\left[1 - \frac{\omega^2}{\omega_{cr2}^2}\cos^4\theta_2 - \frac{\omega_R^2}{\omega^2}\cos^4\beta - \frac{\left(\sigma_x h\cos^2\beta + \sigma_y h\sin^2\beta\right)\cos^2\theta_2}{\rho_s c_2^2}\right]\right\}^2\right)$$

where ω_{cr2} is the critical frequency related to medium 2, ω_R is the ring frequency, m is the surface mass, h is the thickness, c_2 is the speed of sound in medium 2, and $\sigma_x = p_p R/2h$ and $\sigma_y = p_p R/h$. At the critical frequency a resonance condition is created, as the projected wavelength of the sound equals the wavelength of the bending wave in the structure. Another resonance condition occurs at the ring frequency ω_R which equals the ratio of the phase speed of the longitudinal waves in the shell c_{cyl} and the circumference of the shell $2\pi R$.

The field incidence transmission loss of the curved skin was computed by integrating Equation 1 over angles of incidence from 0 to 78 degrees and over azimuth angles from 0 to 360 degrees. The resulting values and the transmission loss for normal incidence are shown in Fig. 8. The figure shows increased transmission loss of the panel at cruise conditions compared to conditions on the ground over the entire frequency range. While the increase in transmission loss below the ring frequency (606 Hz) is modest (less than 5 dB), the transmission loss increase above the ring frequency is significantly more pronounced partially due to an increase in the coincidence frequencies with flow. The coincidence phenomena does not occur for normal incidence and the associated transmission loss is highest of any elevation angle.

4.3 SEA Panel Transmission Loss

The transmission loss of the Q400 fuselage bay section between the ring frames and the longitudinal stringers was also predicted using a script in the commercially available statistical energy analysis program VA-One.[10] The transmission loss of the sidewall (skin, porous layer and trim panel) and the skin by itself were computed. This analysis is not valid below 315 Hz, as the average number of modes in a one-third octave band drops below one. The skin and the trim form a double wall configuration which has a mass-air-mass resonance at 169 Hz for normal incidence. The skin and the trim are assumed to be isolated from one another. Well above this resonance the wavelength is much smaller than the gap between the skin and trim and the total sidewall transmission loss may be predicted by the summation of the transmission loss values of the skin and trim individually.[11]

In order to correct the SEA prediction for pressurization and exterior flow, the components of the transmission loss attributable to the porous layer and trim was added to the previously computed transmission loss for the skin at cruise, which was shown in Fig. 8. The resulting SEA predicted transmission loss for the sidewall (skin, porous layer and trim), corrected for cruise conditions, is shown in Fig. 9.

Below the double wall resonance the wavelength is long compared to the gap between the two panels and the sidewall transmission loss may be predicted from the arithmetic sum of the surface densities of the skin and trim panels. The transmission loss of the total surface density was computed and adjusted for the contribution of the porous layer. The analytically calculated transmission loss of the sidewall is shown in Fig. 9.

4.4 Empirically-based Q400 Sidewall Transmission Loss

Empirically-based transmission loss values for the Q400 sidewall were inferred from the SAE-predicted exterior incident levels and measured interior sound pressure levels[7], with corrections to account for the Q400 noise and vibration system and cabin absorption (Table 4). The predicted incident sound pressure levels in Table 4 correspond to the external sound pressure levels for the Q400 in Fig. 6, minus a 4 dB reflection coefficient that was added by the SAE procedure to account for the presence of the fuselage sidewall. These incident sound pressure levels correspond to the propeller plane, close to the middle of the cabin. Measured one-third octave band interior levels were only available for the front of the cabin, but overall levels were reported in the front as well as in the middle of the Q400 cabin. Hence, the measured one-third octave band frequency spectrum in the front was adjusted for the middle of the cabin by applying the difference between the overall front and mid-cabin levels. These measured interior sound pressure levels are listed in Table 4. The active noise and vibration suppression (NVS) system on the Q400 was operational during the interior noise measurements and was assumed to provide the sound pressure level reductions listed in the NVS column of Table 4 (for the blade passage frequency and first four harmonics). The NVS sound pressure level reductions were added to the measured interior noise levels. Based on the assumption of equal power from each propeller, 3 dB was subtracted from the interior levels to account for the contribution by the second propeller. The noise reduction (NR) of the fuselage sidewall in Table 4 is then defined as the difference in sound pressure levels between the sound incident upon the fuselage and the measured noise in the cabin due to one propeller source without the NVS system active.

The noise reduction of the fuselage sidewall is related to its transmission loss by the average absorption $\bar{\alpha}$ in the cabin[11]

$$NR = TL - 10\log\left(\frac{1}{4} + \frac{S_w(1-\bar{\alpha})}{\bar{\alpha} S_c}\right) \tag{3}$$

where S_w is the sidewall area between the propeller noise source and the cabin interior space and S_c is the total cabin interior surface area. The average absorption coefficient is given by the area-weighted average absorption of several (N) different materials in the cabin[11]

$$\bar{\alpha} = \frac{\sum_{n=1}^{N} S_n \bar{\alpha}_n}{\sum_{n=1}^{N} S_n} \tag{4}$$

Sound absorption coefficients in a realistic cabin mockup are presented in Reference 12 for cabin seats, arm rests, floor and ceiling over a range from 8 Hz to 1000 Hz. The average sound absorption coefficient in the cabin was calculated by determining the surface area for each

different material and applying Equation 4. The resulting average one-third octave band absorption coefficients are listed in Table 5. These values compare well with the sound absorption coefficients measured in a variety of commercial transport aircraft presented in Reference 13. Based on the Reference 13 data a constant average sound absorption coefficient of 0.5 was adopted for the frequency range 1000 Hz to 8000 Hz. The transmission loss of the sidewall is obtained by substituting the average absorption values into Equation 3. The resulting transmission loss is the ratio of the sound power incident on the sidewall and the transmitted sound power, whereby the incident conditions during cruise flight are characterized by outside air density of 0.550 kg/m^3 and speed of sound of 309.7 m/s at 7620 m, and a flow Mach number of 0.60. The receiver side (inside the aircraft cabin) has a density of 0.963 kg/m^3 equal to 2440 m altitude (pressurized 37.9 kPa) and a speed of sound of 340.3 m/s. The relationship in Equation 3 is applicable assuming a diffuse sound field in the cabin. A diffuse field approximation may be valid at frequencies where the wavelength of the sound is small compared to a typical dimension of the cabin cross-section, well away from the cabin boundaries and with no very high absorbing surface inside the cabin. The wavelength at 400 Hz is 0.85 m which is about three times smaller than the 2.69 m diameter of the cabin. The transmission loss values at 315 Hz and below will therefore be less accurate when the noise reduction is corrected for the cabin absorption.

The analytical and statistical energy analysis predictions of the Q400 fuselage sidewall transmission loss at cruise conditions are compared with the semi-empirical estimate in Fig. 9. The semi-empirical estimate is higher than the analytical transmission loss, but agrees well with the SEA prediction where the two overlap (315 – 800 Hz). The analytical transmission loss was predicted for an "infinite" curved panel without stiffeners. However, the longitudinal stringers add stiffness to the fuselage skin thereby increasing the transmission loss in the stiffness controlled region below the ring frequency, as suggested in Reference 14. The ring frames have relatively little effect on the sound transmission loss as the curvature of the panel already provides stiffness and because the distance between the ring frames (0.58 m) is much longer than the distance between the longitudinal stringers (0.124 m)[14]. However, uncertainties in all the parameters used in this initial assessment may preclude definitive conclusions on the cause of any discrepancies.

5 LCTR2 INTERIOR NOISE ASSESSMENT

Although the cruise conditions of the LCTR2 are different from the Q400 (Table 1), for this preliminary assessment the transmission loss trends in Fig. 9 are assumed to describe the behavior of the LCTR2 sidewall without the stiffeners.

Additional low frequency sound transmission is expected where blade passage frequency harmonics couple with the fuselage cross-sectional and longitudinal modes of vibration and the interior acoustic modal resonances. To investigate the structural modal response, a finite element modal analysis was performed on a simple fuselage model. The (bare) fuselage was modeled as a 21.84 m long, floor-equipped aluminum cylinder with 39 evenly spaced ring frames and 68 evenly spaced longitudinal stringers to obtain the structural modal parameters. The trim, windows, overhead bins and chairs were not included in this initial analysis. The lowest four structural cross-sectional modes, which may couple to the interior acoustic space, occur at frequencies ranging from 16.4 to 28.4 Hz. The first longitudinal bending mode of the structure occurred at 15.1 Hz. It is evident that the blade passage frequency and harmonics may excite one or several of these structural resonant modes.

Acoustic interior cross-sectional modes will start at 68 Hz and modes related to the length of the cabin will occur at multiples of 7.8 Hz. Interior noise levels will peak when the excitation frequencies of the rotor noise coincide with the structural and/or acoustic modal resonances. At these resonance frequencies passive or active damping control may be most effective. Active structural control will need sizable structural displacements and associated power to be successful at these low frequencies. For active acoustic control fewer sensors and activators will be required because of the long wavelengths, although it may be challenging to generate ample acoustic power to control the noise efficiently by a lightweight system.

Considering the predicted unweighted sound pressure levels of the LCTR2 in Fig. 6 and the transmission loss estimates of the notional sidewall in Fig. 9, the low frequency cabin interior noise may approach levels (130 dB at the 6.9 Hz blade passage frequency and more than 110 dB for the first three harmonics) that are not acceptable to the occupants of the tiltrotor cabin[15]. The problem may be augmented by the use of lightweight composite and sandwich materials for the fuselage of future tiltrotor vehicles which may provide less transmission loss than the conventional metal fuselage structure. Not only the level but also the character of the noise is important. Periodic low frequency variations induced by the aerodynamic pressure pulses of the rotor blades may produce annoying modulation of the noise inside the cabin[15]. More accurate predictions of the exterior noise levels, sidewall transmission loss, and interior acoustic environment of the tiltrotor cabin will be undertaken to more precisely assess LCTR2 interior noise, and aid in identifying and evaluating noise control strategies.

6 CONCLUSIONS

A preliminary assessment was made of the expected interior noise environment in the LCTR2 cabin. Sound pressure levels incident on the LCTR2 fuselage due to the rotor harmonics during cruise were predicted using an empirical procedure for near-field propeller noise. Sound transmission loss values for a fuselage sidewall assumed to resemble that of the Bombardier Q400 were computed using simple analytical expressions at low frequencies and statistical energy analysis above 315 Hz. The SEA predictions agreed well with empirically-based estimates of the sidewall transmission loss from 315 to 800 Hz, but the analytical predictions underestimated the empirical sidewall transmission loss at the low frequencies. Structural and acoustic resonances are expected to coincide with low order harmonics of the blade passage frequency. The assumptions and inaccuracies in these initial analyses highlight the need for more precise models to assess the noise reduction at the very low frequencies relevant to the LCTR2. The high interior noise levels obtained by combining the predicted exterior noise levels and the estimated transmission loss of a notional sidewall indicated that the low frequency interior sound pressure levels may be objectionable to passengers. Using lightweight composite and sandwich materials for the fuselage sidewall, having even lower transmission loss than estimated here, could exacerbate the interior noise problem.

7 REFERENCES

1. Johnson, W., Yamauchi, G. K., and Watts, M. E. NASA Heavy Lift Rotorcraft Systems Investigation. NASA TP-2005-213467, September 2005.

2. Acree, C. W., Yeo, H., and Sinsay, J. D. Performance Optimization of the NASA Large Civil Tiltrotor. International Powered Lift Conference, London, UK, July 2008; also NASA TM-2008-215359, June 2008.

3. Acree, C. W. Jr. Integration of Rotor Aerodynamic Optimization with the Conceptual Design of a Large Civil Tiltrotor NASA Ames Research Center Report Number: ARC-E-DAA-TN1176, January 2010.

4. Aviation International News. - Bombardier considers stretch variant for Q400. Paris Air Show. Air Transport and Cargo Aircraft. June 2009.

5. Society of Automotive Engineers - SAE Technical Standards: Prediction Procedure for Near-Field and Far-Field Propeller Noise. SAE International – Aerospace Information Reports, SAE AIR 1407-1977 (Reaffirmed: April 1991).

6. Lyle, Karen H. XV-15 Structural-Acoustic Data. NASA Technical Memorandum 112855, U.S. Army Research Laboratory Technical Report 1423, June 1997.

7. Tubbs, Randy L. NIOSH Health Hazard Evaluation Report HETA 2002-0354-2931. Horizon Air. Seattle, Washington. February 2004.

8. Gardonio, P. and Gonzalez Diaz, C. Bombardier Dash-8 Q400 Fuselage Section with Five Decentralized Velocity Feedback Control Units. ISVR Technical Memorandum 983. Institute of Sound and Vibration Research, Southampton, United Kingdom, January 2009.

9. Koval, L. R., "Effect of Air Flow, Panel Curvature, and Internal Pressurization on Field-Incidence Transmission Loss," Journal of the Acoustical Society of America, Vol. 59, No. 6, 1976, pp. 1379–1385.

10. ESI Group. VA One Virtual TL Module – User's Guide and Theory. June 2010.

11. Beranek, L. L., ed., *Noise and Vibration Control*. New York: McGraw-Hill, 1988.

12. Mallardo, Vincenzo and Aliabadi, Ferri M.H. Noise Control by BEM in Large Scale Engineering Problems. Paper 267. XIX AIMATA Congress, Italian Association for Theoretical and Applied Mechanics, Ancona, Italy, 14-17 September 2009.

13. Wilby, J. F., Rennison, D. C. and Wilby, E. G. Noise Control Predictions for High-Speed, Propeller-Driven Aircraft. AIAA-80-0999, AIAA 6th Aeroacoustics Conference, Hartford, Connecticut, 4-6 June 1980.

14. Liu, B. L., Feng, L. P., and Nilsson, A., "Sound Transmission Through Curved Aircraft Panels with Stringer and Ring Frame Attachments," Journal of Sound and Vibration,Vol. 300, No. 3–5, Mar. 2007, pp. 949– 973.

15. Fidell, Sanford, Horonjeff, Richard D. and Schmitz, Fredric H. Research Plans for Improving Understanding of Effects of Very Low-Frequency Noise of Heavy Lift Rotorcraft. NASA/CR-2010-216203, February 2010.

Table 1. Design parameters for the LCTR2, the Bombardier Q400 and the Bell XV-15.

Parameter		**LCTR2**	**Q400**	**XV-15**
Fuselage diameter	[m]	2.74	2.69	
Maximum cabin width	[m]	2.56	2.51	1.52
Cabin length	[m]	21.84	18.80	3.99
Passengers		90	78/90	8
Maximum cruise speed	[km/hr]	556	667	481
Maximum operating altitude	[m]	8534	7620	8992
Number blades		4	6	3
Tip speed cruise	[m/s]	107	182.9	206.3
BPF cruise	[Hz]	6.9	85	25.84
RPM cruise	[rpm]	117.5	850	517
Rotor radius	[m]	9.906	2.055	3.81
Clearing rotor tip-fuselage	[m]	0.457	1.00	0.259

Table 2. Mechanical properties of the honeycomb trim panel core.

Material layer	**ρ** [kg/m^3]	**E_{11}** [GPa]	**E_{22}** [GPa]	**E_{33}** [GPa]	**G_{12}** [GPa]	**G_{23}** [GPa]	**G_{31}** [GPa]	**ν_{12}** [-]	**ν_{23}** [-]	**ν_{31}** [-]
Core	48.16	0.031	0.031	0.138	0.000138	0.0235	0.0448	0.20	0.20	0.045

Table 3. Material properties of the acoustic absorptive material.

ρ [kg/m^3]	**m** [kg/m^2]	**t** [mm]	**E** [Pa]	**ν** [-]	**σ** [Ns/m^4]	**φ** [-]	**α_∞** [-]	**Λ** [mm]	**Λ'** [mm]	**η** [-]
8.8	0.447	50.8	80000	0.4	10900	0.99	1.02	0.1	0.13	0.17

Table 4. Q400 fuselage sidewall transmission loss calculation in the propeller plane for cruise flight conditions.

One-third octave band center frequency [Hz]	**Predicted incident SPL [dB]**	**Measured interior SPL [dB]**	**Noise and Vibration Suppression (NVS) [dB]**	**Fuselage sidewall NR [dB]**	**Fuselage sidewall TL [dB]**
80	124.0	91.8	11.3	23.9	26.6
100		74.5			
125		72.8			
160	122.5	78.7	17	29.8	28.3
200		72.6			
250	120.5	83.1	6.6	33.8	31.7
315	119.0	71.6	3.5	46.9	44.5
400	117.0	71.6	0.8	47.6	44.7
500	115.5	72.3		46.2	42.9
630	116.7	73.5		46.2	42.7
800	115.6	75.8		42.9	39.2
1000	116.6	77.3		42.3	38.3

Table 5. Q400 cabin estimated average sound absorption coefficients.

One-third octave band frequency [Hz]	Average sound absorption coefficient [-]	One-third octave band frequency [Hz]	Average sound absorption coefficient [-]
8	0.018	100	0.151
10	0.019	125	0.284
12.5	0.021	160	0.307
16	0.021	200	0.331
20	0.025	250	0.358
25	0.030	315	0.390
31.5	0.034	400	0.430
40	0.040	500	0.481
50	0.057	630	0.507
63	0.086	800	0.536
80	0.114	1000	0.578

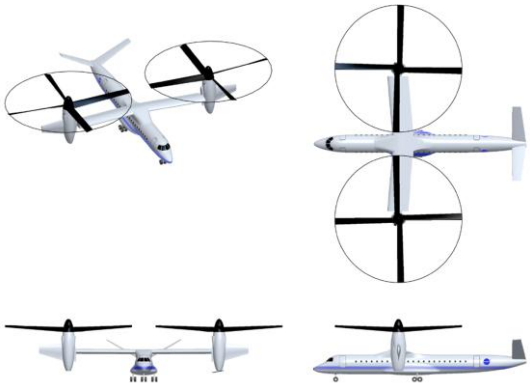

Fig. 1 - Isometric and three-view of the Large Civil Tiltrotor (LCTR2) design.

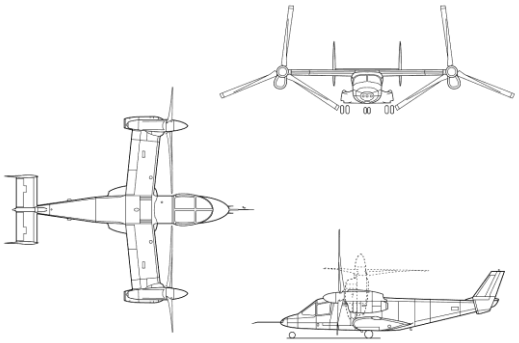

Fig. 2 - Three-view of the Bell XV-15 tiltrotor.

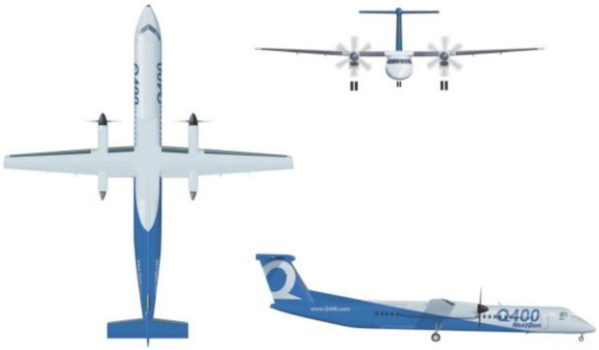

Fig. 3 - Three-view of the Bombardier Q400 turboprop airliner (http://Q400.com).

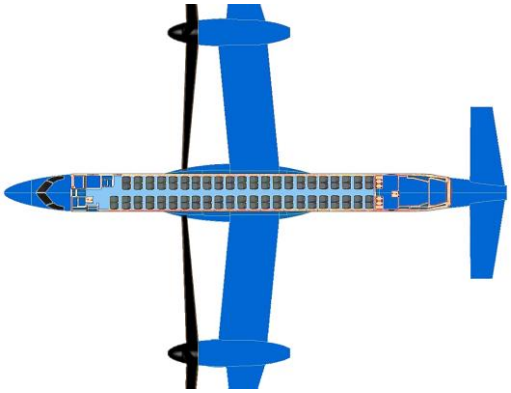

Fig. 4 - Sketch of a hypothetical LCTR2 90-passenger seating layout.

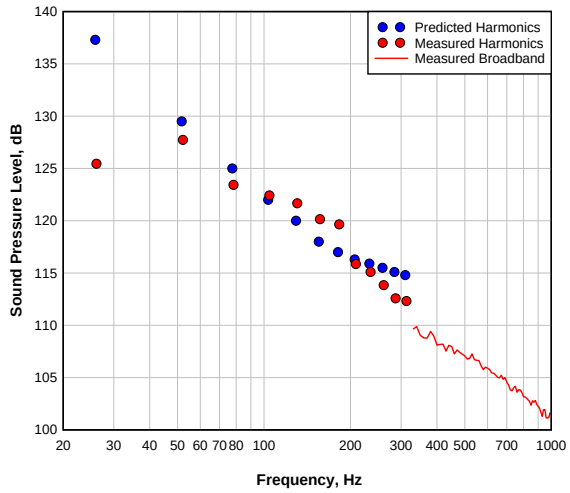

Fig. 5 – The predicted and measured XV-15 sound pressure levels at the fundamental rotor blade passage frequencies and the first eleven harmonics for cruise flight conditions.

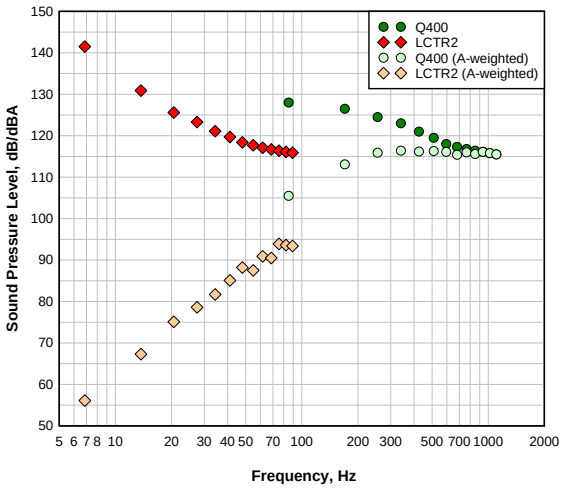

Fig. 6 –Predicted un-weighted and A-weighted sound pressure levels of the Q400 and LCTR2 flight vehicles at the fundamental frequency and the first twelve harmonics for cruise flight conditions.

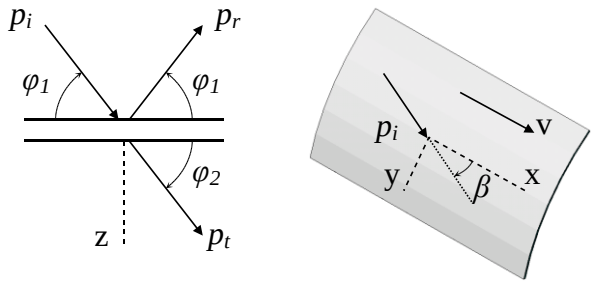

Fig. 7– Elevation angle ϕ_1 and azimuth angle β between the incoming pressure wave p_i and the panel structure and the elevation angle ϕ_2 for the transmitted wave.

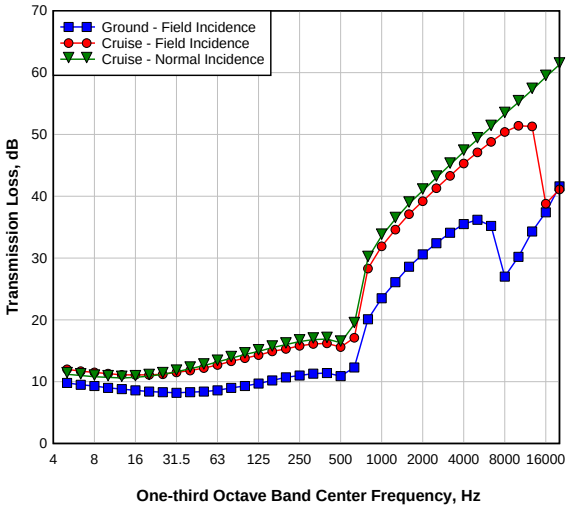

Fig. 8– Analytical sound transmission loss predictions of the Q400 aircraft skin at the ground or in cruise flight conditions.

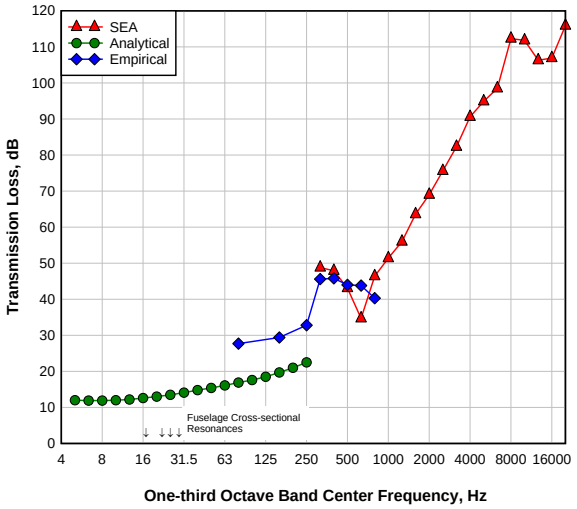

Fig. 9– Analytical, statistical energy analysis, and semi-empirical sound transmission loss predictions for the Q400 sidewall during cruise conditions.